Science of the Total Environment 664 (2019) 824–833

Contents lists available at ScienceDirect

Science of the Total Environment

journal homepage: www.elsevier.com/locate/scitotenv

Response of streamflow to environmental changes: A Budyko-type analysis based on 144 river basins over China

Yanzhong Li [a], Changming Liu [a,b], Wenjun Yu [a,*], Di Tian [c], Peng Bai [b]

[a] School of Hydrology and Water Resources, Nanjing University of Information Science & Technology, Nanjing 210044, China
[b] Institute of Geographic Sciences and Natural Resources Research, Chinese Academy of Sciences, Beijing 100101, China
[c] Department of Crop, Soil and Environmental Sciences, Auburn University, AL 36849, USA

HIGHLIGHTS

- Bias correction to precipitation and optimization to a_s and b_s are essential for aridity index application
- Streamflow is more sensitive to climate change in water-limited region than that in equitant and energy-limited region
- Streamflow is dominated by climate in energy-limited and equitant regions and by other factors in water-limited region

GRAPHICAL ABSTRACT

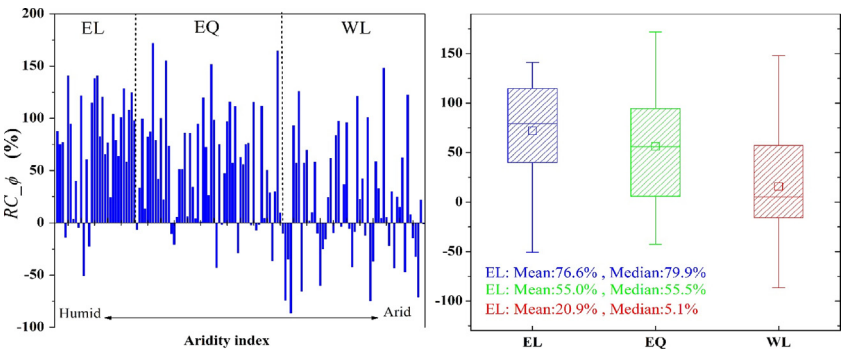

ARTICLE INFO

Article history:
Received 7 November 2018
Received in revised form 26 January 2019
Accepted 1 February 2019
Available online 2 February 2019

Editor: Ouyang Wei

Keywords:
Aridity index
Budyko analysis
Climate regions
Environmental change
Sensitivity analysis

ABSTRACT

Understanding response of streamflow to environmental changes is crucial for large-scale water resources management and ecosystem restoration. There is no consensus on how environmental change influence streamflow in different regions across climate gradient, as previous studies mainly focused on a single river basin or climate region. This study analyzed the variations of aridity index and its contributions to streamflow change based on Budyko's framework approach using bias-corrected precipitation measurement, parameters-optimized potential evapotranspiration and observed streamflow in 144 basins across China. The parameter *n* in the Budyko type equation exhibits significant spatial heterogeneity, with larger values in the water-limited region than in the energy-limited region, which suggests more pronounced impact of basin characteristic or vegetation change on hydrological cycle. The absolute value of sensitivity coefficient in the water-limited region (−2.56) was larger than both equitant (−2.13) and energy limited region (−1.57), indicating that the streamflow was more sensitive to aridity index change in the water-limited region than in the equitant and energy-limited regions. The dominant factor affecting streamflow under energy-limited and equitant conditions is aridity index (i.e. climate change), with median relative contribution rates of 79.9% and 55.5%, respectively. In contrast, non-climatic factors dominate the variation of streamflow in the water-limited region, the effect of climate change on streamflow has been offset by other factors. This study suggests that the water management practices, such as water diversion across river basins and ecological restorations, should fully consider the differences in hydrological responses to climatic conditions.

© 2019 Elsevier B.V. All rights reserved.

* Corresponding author.
E-mail address: wj.yu@nuist.edu.cn (W. Yu).

https://doi.org/10.1016/j.scitotenv.2019.02.011
0048-9697/© 2019 Elsevier B.V. All rights reserved.

1. Introduction

Environmental changes, such as climate changes and the changes induced by human activity is unequivocal and particularly remarkable over the past three decades (NOAA, 2018; IPCC, 2013). The hydrological cycle has been accelerated (Donat et al., 2016; Piao et al., 2010; Ohmura and Wild, 2002; Zhang et al., 2018a) and exhibited large spatial and temporal heterogeneity due to the environmental change (Greve et al., 2014). In particularly, the widely spread concept that dry regions become drier and wet regions become wetter as climate change could be severed as a simplified summary of regional different response to the changing environment (Held and Soden, 2006). In addition, the global warming hiatus (Medhaug et al., 2017) has caused a wetting trend over the mid-to-high latitude regions of Eurasia and Greenland, but a drying trend in over North America, southern Europe and eastern China (Guan et al., 2017). Regional response differences to environmental change introduces great challenge to the hydrological cycle study and water resources management (Jaramillo and Destouni, 2015; Kang and Eltahir, 2018; Wang et al., 2019; Xing et al., 2018).

Aridity index (ϕ), defined as the ratio of annual potential evapotranspiration (*PET*) to precipitation (*P*), is a highly suitable way to aggregate complex climate gradients into a simple but hydrometeorological meaningful indicator (UNESCO, 1979). The aridity index has been widely used for dividing climatic zones (Maliva and Missimer, 2012; McVicar et al., 2012) and assessing the impact of climate change on hydrological cycle (Roderick et al., 2015; Yang et al., 2018; Zhang et al., 2016). Studies showed that the aridity index increased by human-induced climate change (Kang and Eltahir, 2018; Cook et al., 2014), and significantly reduced water supply in different climate regions (Roderick et al., 2015; Liu et al., 2013; Liang, 2018). At the global scale, some researchers argue that the aridity index over land surface would increase significantly leading to water scarcity, particularly in the tropics, subtropics, and midlatitudes regions (Scheff and Frierson, 2015). While some other researchers argue that although the aridity index would be increased in most global basins, the streamflow (*Q*), as one of the key components in water cycle, could also be increased in the future due to its varied levels of sensitivities to *PET* and precipitation (Yang et al., 2018; Yang et al., 2019), particularly in the water-limited regions (Berghuijs et al., 2017). At the regional scales, while the aridity index would be increased in equitant and water-limited regions, it demonstrated remarkablely different contributions to streamflow, with the values of 68.8% and 31.5%, respectively (Liu et al., 2013). Investigating the responses of streamflow to aridity index in different climatic regions is vital for understanding the effects of climate change on water resources in river basins and for implementing adaptation strategies of climate change for regional water resources management. As previous studies primarily focus on a single river basin or climate region, there is no consensus on how climate influence streamflow in different climatic regions. Comprehensively assessing the responses of streamflow to aridity index would be of great importance for a better understanding of the differences in regional hydrologic responses on climate change and therefore for improving region-specific adaptive strategy-making in response to climate change. However, to the best of our knowledge, such assessment is still lacking in the current literature.

China covers a wide temperature gradient decreasing from south to north, and a large precipitation gradient decreasing from southeast to northwest, which provides an ideal case for such assessment. In this study, we selected 144 basins in China and classified them into three climatic regions to examine the impacts of aridity index on streamflow under the changing environment. The specific objectives of this study are to: (1) investigate the spatial distribution and significance of parameter *n* in Budyko type equation in three climatic regions, (2) evaluate the sensitivity of streamflow to aridity index in different climate regions, and (3) assess the influence of aridity index on streamflow under the changing environment.

2. Study area and data

2.1. Study area

We selected 144 basins to investigate the impact of climate change on hydrological responses. These basins cover a broad geographic and climatic conditions (Fig. 1). The area of basins spans from 385 to 137,704 km^2. The mean annual air temperature ranges from −5 to 22 °C. The mean annual precipitation ranges from 343 to 2628 mm. The mean annual potential evapotranspiration (*PET*) spans from 652 to 1645 mm. The runoff depth ranges from 7.5 to 2410 mm. The aridity index (ϕ) spans from 0.53 to 3.67. The 144 basins were grouped into three climate regions based on the aridity index: energy-limited ($\phi \le 0.76$), equitant ($0.76 < \phi \le 1.35$) and water-limited conditions ($\phi > 1.35$) (McVicar et al., 2012). The basic hydrological and climatological characteristics were summarized in Table 1.

2.2. Data

The monthly observed streamflow data from 144 hydrological stations (Fig. 1) were obtained from the Hydrological Bureau of China. The daily meteorological records, including precipitation, temperature, relative humidity, and wind speed at 10 m, from 742 national meteorological stations were collected from the National Climatic Center of China Meteorological Administrator (http://data.cma.cn/), covering the period of 1960–2000. The missing precipitation, relative humidity and wind speed are filled with the values from the nearest station, while the missing temperature is filled with the averaged values of previous and next days. The wind speed was adjusted to 2 m height (U_2) using the wind profile and height relationship (Allen et al., 1998).

As one of key inputs for calculating aridity index, reliable precipitation data are essential for quantifying the impact aridity index on streamflow. However, biases in precipitation have been widely recognized due to station distribution, observational techniques and gauge measurement error (Ye et al., 2004; Yang et al., 2001; Goodison et al., 1989). Such biases in precipitation can bring significant uncertainties in simulating and projecting water resources availability (Liu et al., 2017; Sorooshian et al., 2011). Therefore, correction to the gauged precipitation data is of great necessity before applying the data for aridity index calculation (Li et al., 2017; Liu et al., 2016). To correct the gauged precipitation, the WMO Solid Precipitation Measurement Intercomparison has developed several bias-correction techniques for various precipitation gauges commonly used around the world (Goodison et al., 1989). In China, Ye et al. (2004) conducted a bias-correction approach to precipitation and found wind-induced gauge undercatch is the greatest measurement error in precipitation in most regions, followed by wetting loss. The wetting loss refers to the precipitation being retained or stuck on the sides of the gauge, and could not be poured out and measured in the precipitation observation. The wind-induced undercatch of precipitation refers to the deformation of wind field above the gauge orifice (Sevruk and Hamon, 1984). Therefore, we also mainly corrected these two kind errors as follows.

Correction to measurement error in precipitation was conducted by the following Eq. (1):

$$P_c = \frac{(P_g + \Delta P_w)}{CR} \quad (1)$$

where P_c represents the bias-corrected precipitation based on precipitation types (rain, snow, and mixed precipitation) (Ye et al., 2004); P_g is the gauge record; ΔP_w is the wetting loss. *CR* is the catch ratio, which is defined as the ratio of gauge measured precipitation to the true precipitation (Goodison et al., 1989). The smaller value of *CR* indicates larger precipitation bias. Fig. 2a shows that *CR* ranges from 0.81 to 0.97, with the average of 0.91, which indicates that the gauge records can cause error by 3% to 19% in the 144 basins. For example, in the Beijing station, the annual mean precipitation of gauge and corrected are 573.8 mm and

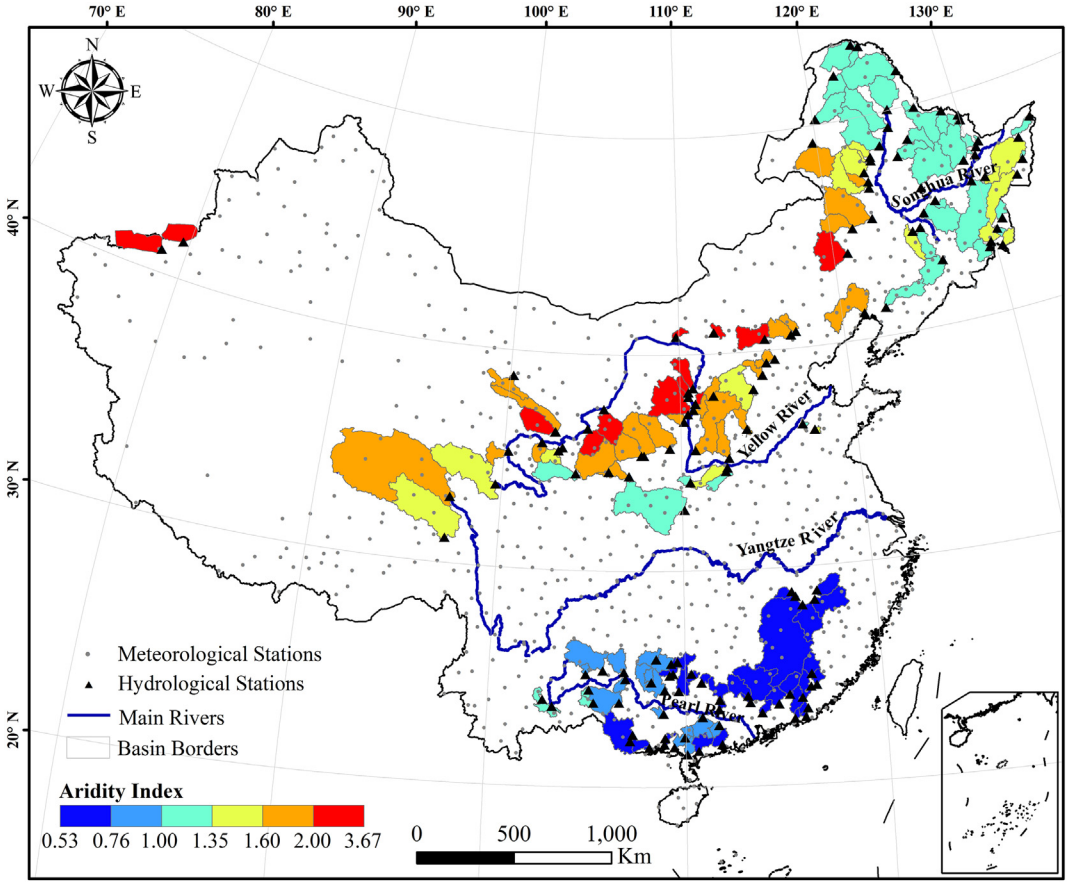

Fig. 1. Distribution of 144 basins selected in the study. The triangles represent the outlets of each basin and the gray dots represent the meteorological stations.

647.1 mm, respectively, during 1960–2000, accounting for 12.8% of gauge precipitation (Fig. 2b). Thus, without bias correction, the precipitation would be largely underestimated compared with observational precipitation, and it could cause a higher aridity index and overestimation of the impact of aridity index on streamflow, and finally obtain an incorrect conclusion. The bias-correction to the precipitation in this study can ensure the precision of calculating aridity index and water balance application.

3. Methods

3.1. Estimating potential evapotranspiration

The Potential evapotranspiration (*PET*) is estimated by the Penman (1948) as follows:

$$PET = \frac{\Delta}{\Delta+\gamma}(R_n - G) + \frac{\gamma}{\Delta+\gamma}[0.26(1+0.52U_2)](e_s - e_a) \quad (2)$$

where *PET* is the potential evapotranspiration (mm d^{-1}), Δ is the slope of saturated vapor pressure in relation to air temperature (kPa·°C^{-1}); γ is the psychrometric constant (kPa·°C^{-1}); R_n is the net radiation (MJ m^{-2} d^{-1}), and G is the soil heat flux density (MJ m^{-2} d^{-1}); U_2 is the wind speed at the 2 m height (m s^{-1}); e_s and e_a are the saturation and actual vapor pressure (kPa), respectively.

The net radiation R_n, *as* the key variable for calculate *PET*, can be obtained from the difference between net shortwave radiation (R_{ns}) and net long-wave radiation (R_{nl}).

$$R_n = R_{ns} - R_{nl} \quad (3)$$

$$R_{ns} = (1-\alpha)R_s = (1-\alpha)\left(a_s + b_s\frac{d_s}{N}\right)R_a \quad (4)$$

where α is the albedo of reference grassland ($\alpha = 0.23$), d_s is the actual duration of sunshine (hours), N is the maximum possible duration of sunshine or daylight hours (h) (d_s/N is the relative sunshine duration),

Table 1
Descriptions of the 144 basins in three climate regions in China.

	Area (km^2)	P (mm yr^{-1})	PET (mm yr^{-1})	ϕ	Q (mm yr^{-1})
EL	10,645	1923	1301	0.68	1095
($n = 32$)	(441–80,948)	(1606–2628)	(1175–1645)	(0.53–0.76)	(628–2410)
EQ	9688	958	989	1.11	332
($n = 55$)	(385–59,115)	(520–1846)	(652–1417)	(0.77–1.35)	(56–843)
WL	15,165	532	946	1.82	91
($n = 57$)	(1121–137,704)	(343–760)	(757–1094)	(1.36–3.67)	(8–375)

Notes: EL, EQ and EL refer to the energy-limited, equitant and water-limited environment, and the number after the abbr. represents the count of basins. *P* refers to the annual precipitation. *PET* refers to the potential evapotranspiration. ϕ refers to the aridity index, defined as the ratio of *PET* to *P*. *Q* refers to the runoff depth.

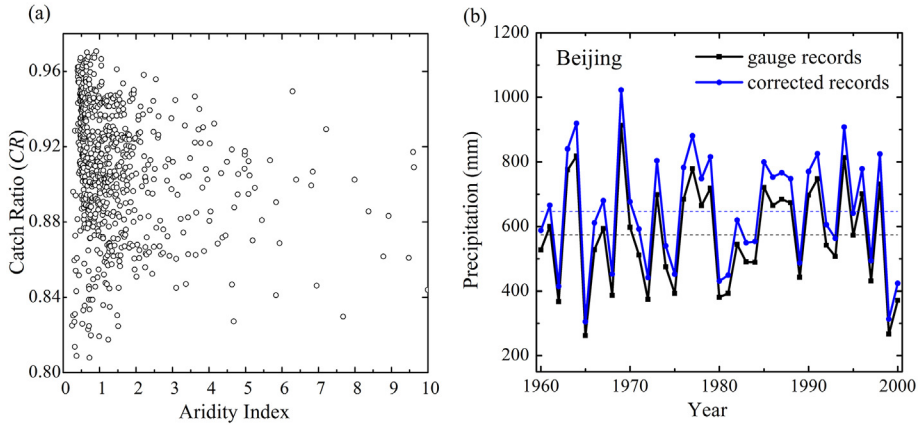

Fig. 2. Correction to gauge measured error in precipitation from the 742 meteorological stations. (a) average value of catch ratio (*CR*) of the gauge measured precipitation to the bias-corrected precipitation. (b) the difference between gauged and bias-corrected annual precipitation from 1960 to 2000 for Beijing station.

and R_a is the extraterrestrial radiation intensity (MJ m^{-2} d^{-1}). The coefficients a_s and b_s were set as constant ($a_s = 0.25$, $b_s = 0.50$) in the Food and Agriculture Organization (FAO) 56 document (Allen et al., 1998). In fact, these two coefficients vary with locations and were re-calibrated by an optimized method using the data from solar radiation stations (Liu et al., 2012a).

Fig. 3 shows significant spatial heterogeneity in a_s and b_s, with a_s ranging from 0.12 to 0.29 and b_s from 0.45 to 0.74. The spatial heterogeneity of these two coefficients suggests the necessity of using the optimized values instead of the constant, since the optimized a_s and b_s values will improve the estimation of *PET* and reduce uncertainties in the following analysis.

3.2. Sensitivity analysis and contribution of aridity index to streamflow

The sensitivity coefficient, defined as the ratio of the change rate of dependent variable to the change rate of some independent variables, has been used as an effective indicator to reflect streamflow sensitivity to change in other variables, such as the *PET*, *P* and ϕ (Zheng et al., 2009). The sensitivity of streamflow to aridity index can be expressed as follows:

$$S_\phi = \lim_{\Delta\phi/\phi \to 0} \left[\frac{\Delta Q/Q}{\Delta\phi/\phi}\right] = \frac{\partial Q}{\partial \phi} \times \frac{\phi}{Q} \tag{5}$$

According to the definition, a positive (negative) sensitivity coefficient indicates that an increase (decrease) in the aridity index will bring an increase (decrease) in streamflow. If the S_ϕ is equal to 0.1, which means that a 10% increase of aridity index would lead to an increase in streamflow of 1%.

In a closed basin, the water balance can be expressed as:

$$P = Q + ET_a + \Delta S \tag{6}$$

where ET_a is the actual evapotranspiration (mm yr^{-1}); ΔS is the terrestrial water storage change (mm yr^{-1}), which reflects the changes in the moisture storage in surface and subsurface stores, such as glaciers, groundwater, and soil moisture. For a long-term period (e.g., 10 years or more), the water storage change can be assumed zero (Hobbins et al., 2001), then the Eq. (6) can be rewritten as:

$$P = Q + ET_a \tag{7}$$

According to the Budyko hypothesis (Budyko, 1974), evapotranspiration index (ET_a/P) is regarded as an indicator of the long term mean annual water balance in a basin, and the mean annual evapotranspiration (ET_a) is mainly controlled by available energy (*PET*) and available water (*P*). Since the aridity index (ϕ) is a ratio of *PET* to *P*, ET_a/P can be expressed as a function of ϕ (Ye et al., 2015; Zhang et al., 2001; Yang

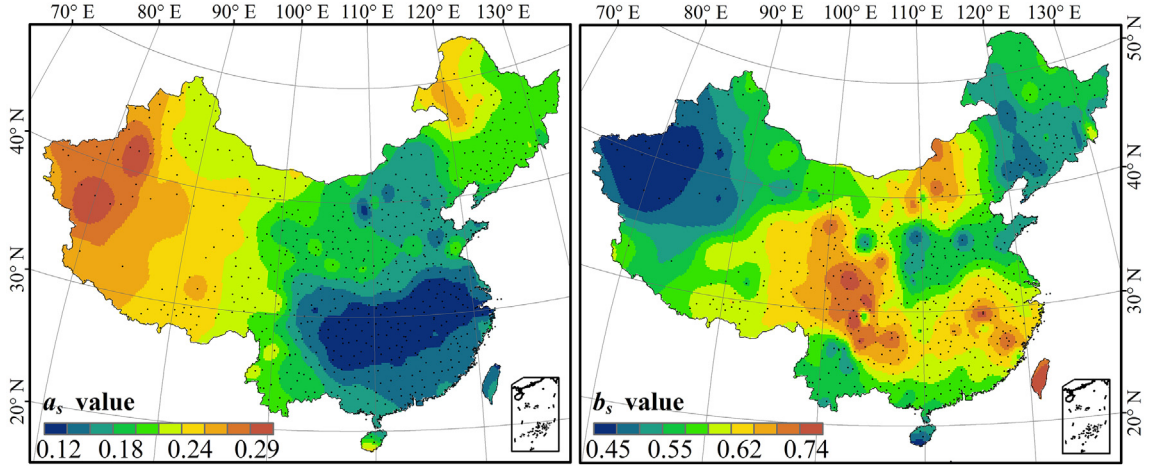

Fig. 3. Distribution of optimized parameter a_s and b_s for calculating solar radiation in China. (a) The distribution of parameter of optimized a_s and (b) b_s. The gray dots represent the meteorological stations.

et al., 2008):

$$\frac{ET_a}{P} = F(\phi) \tag{8}$$

Combined Eqs. (7) and (8), the annual streamflow can be evaluated by:

$$Q = P - P \times F(\phi) = P \times (1 - F(\phi)) \tag{9}$$

The partial derivative of Q to ϕ can be expressed as:

$$\frac{\partial Q}{\partial \phi} = -\frac{P^2}{PET}(1 - F(\phi)) - P \times F'(\phi) \tag{10}$$

Thus, the sensitivity of streamflow to aridity index can be obtained based on Eqs. (5) and (10):

$$S_\phi = -\frac{P}{Q}(1 - F(\phi)) - \frac{PET}{Q} F'(\phi) \tag{11}$$

The Choudhury-Yang Equation is used for estimating $F(\phi)$ and $F'(\phi)$ based on the Budyko framework (Yang et al., 2008; Yang and Yang, 2011), as follows:

$$F(\phi) = \frac{1}{\left(1 + \phi^{-n}\right)^{1/n}} \tag{12}$$

$$F'(\phi) = \frac{1}{\phi^{n+1}\left(1 + \phi^{-n}\right)^{1+1/n}} \tag{13}$$

where parameter n is dimensionless and is related to the basin characteristic, such as vegetation condition, soil properties and landscape. Researches indicate that n could effectively reflect the plant condition in a basin, and a strong relationship existed between the change in the landscape parameter n and vegetation change (Zhang et al., 2015; Liang et al., 2015; Zhang et al., 2018b).

The contribution of change in aridity index to streamflow (Cr_ϕ) and the relative contribution rate (RC_ϕ) can be evaluated as:

$$Cr_\phi = S_\phi \times \Delta\phi \times 100\% \tag{14}$$

$$RC_\phi = \frac{Cr_\phi}{\Delta Q} \times 100\% \tag{15}$$

3.3. Statistical and spatial analysis

The spline method in the spatial analysis toolbox of ArcGIS 10.2 was used to obtain the spatial distribution of various hydrological and climate factors, and then the values of 144 basins were extracted by Python2.7. The one-way analysis of variance (ANOVA) and the Mann-Whitney U test in SPSS 20.0, were used to test the significant differences in the mean and medians of parameter n and sensitivity of annual streamflow to aridity index for three climate regions.

The Mann-Kendall statistical test (Kendall, 1948) was employed to detect the trend in annual aridity index and streamflow (Li et al., 2016; Liu et al., 2011), due to its robustness for non-normally distributed data. Assuming a normal distribution at the significant level of $p = 0.05$, a positive Mann-Kendall statistic Z larger than 1.96 indicates a significant increasing trend, whereas a negative Z lower than −1.96 indicates a significant decreasing trend. Critical Z values of ±1.64, ±2.58, and ±3.29 were used for the probabilities of $p = 0.1$, 0.01, and 0.001, respectively.

4. Results

4.1. Parameter n in the Budyko framework under different climatic regions

Fig. 4 shows the relationship of aridity index (ϕ) and evapotranspiration index (ET_a/P) in the three climatic regions. The results indicate that the small values of ϕ ($\phi \to 0$) are found in humid basins, where the water is sufficient, and the energy supply is the key limiting factor for evapotranspiration; the large values of ϕ ($\phi \to 0$) are associated with arid regions where the precipitation is scarce, and the water supply is the limiting factor for evapotranspiration. Our findings are generally consistent with the Budyko's framework, which shows that the humid basins are located in the energy-limited area (blue dot, smaller ET_a/P), sub-humid and semi-arid basins in the equitant area (Green triangle, medium ET_a/P) and arid basin in the water-limited area (red square, larger ET_a/P). The parameter n in Choudhury-Yang model (Eq. (12)) can effectively reflects the combined influences of various catchment characteristics such as soil, vegetation, and climatic conditions. The larger value of n means the greater ratio of ET_a to precipitation (Zhang et al., 2015; Fan et al., 2017). When different values of parameter n were set, we can get similar curve to "Budyko Curve" (Fig. 4). The parameter n in the 144 basins were calibrated by mimimizing the difference between long-term ET_a estimates from Eq. (12) and water balance based ET_a ($ET_a = P$-R). Fig. 5a shows the distribution of parameter n in 144 basins. The parameter n values exhibit significant spatial heterogeneity. The smaller n values in southeast and northeast China are mainly in the humid and sub-humid regions, while the larger n values are in the semi-arid and arid regions (Fig. 1), which indicates that the streamflow could suffer from greater influence of basin or vegetation change in the arid region than that in the humid region (Zhang et al., 2015).

Fig.5b shows the statistic of parameter n in energy-limited, equitant and water-limited regions. The energy-limited basins have the lowest average n 1.28 (10th percentile, 0.31; 90th percentile, 2.65) and coefficient of variation (CV) value 48%; In the equitant basins, the mean n is larger than that in energy-limited regions and smaller than water-limited regions, with the mean value of 1.79 and median value of 1.56 (10th percentile, 0.94; 90th percentile, 2.42); the parameter n in water-limited regions is the largest, with mean value of 2.04, median value of 2.03 (10th percentile, 0.67; 90th percentile, 3.44) and CV value of 35%. The one-way ANOVA and the Mann-Whitney U tests (Table 2) demonstrate significant difference of mean and median parameter n between any two of three climate regions ($p < 0.05$), except for equitant and water-limited region with ANOVA test ($p > 0.05$). In particular, the statistical test results of parameter n between energy-

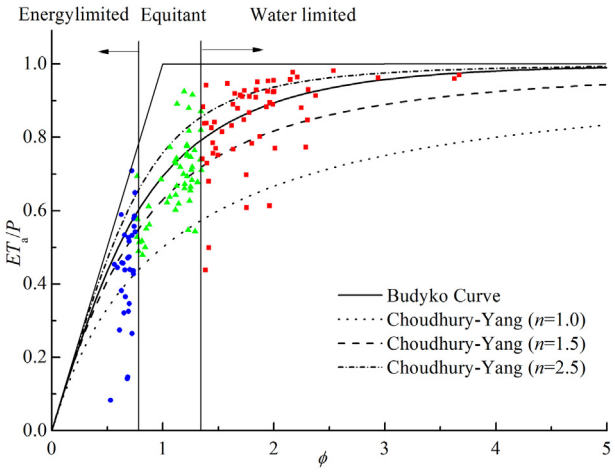

Fig. 4. Budyko and Choudhury-Yang curve relating the evapotranspiration ratio (ET_a/P) to the aridity index (ϕ) in three climate regions of the 144 basins in China.

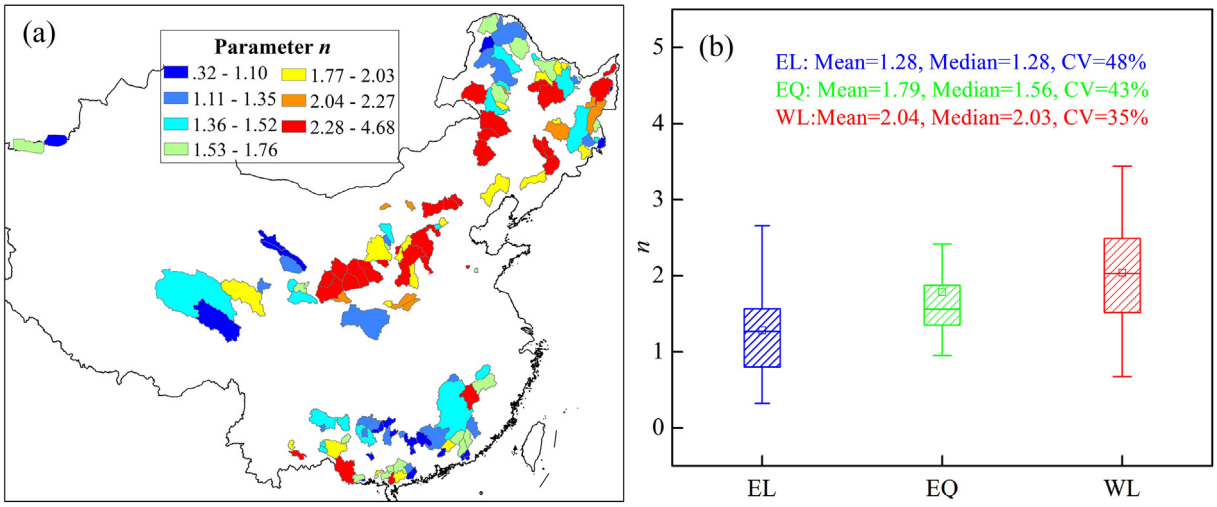

Fig. 5. (a) Distribution parameter *n* in 144 basins and (b) comparison on parameter n grouped by energy-limited (EL), equitant (EQ) and water-limited (WL) regions.

limited and water-limited conditions reach the highest significant level ($F = 25.69, Z = 4.677, p < 0.000$), which indicates that the basin characteristics (such as basin area, soil, vegetation type and density) exert different impact on streamflow. Additionally, the drier a basin is, the more pronounced the impact of basin characteristic or vegetation change on hydrological cycle and vice versa.

4.2. Sensitivity of streamflow to aridity index

Fig. 6 shows the spatial distribution of sensitivity coefficient (S_ϕ) in 144 basins and the statistical test grouped by three climate conditions. The smaller absolute values of S_ϕ mainly occurred in the Pearl river basin, where annual precipitation is also the highest (Fig. 6a). The larger absolute values of S_ϕ happened in the middle region of China, especially in the middle Yellow River basin (Figs. 1 and 6a), where belongs to semi-arid or arid regions with low annual precipitation. The result suggests that the streamflow is more sensitive to aridity index in arid river basins than that in humid river basins.

The smallest absolute value of mean S_ϕ (−1.57; 10th percentile, −2.56; 90th percentile, −1.05) occurred in the energy-limited regions, with a median value of −1.54 and *CV* value of −23%. In the equitant condition, the mean S_ϕ is −2.13 (10th percentile, −2.71; 90th percentile, −1.50), with a median value of −1.91 and *CV* value of −31%. The most sensitive responses of streamflow to ϕ was found in water-limited regions, with a mean value of −2.65(10th percentile, −4.44; 90th percentile, −1.71), a median value of −2.66 and a *CV* value of −29%. It indicates that a 10% increase of ϕ in EL, EQ and WL regions could cause a decrease of streamflow by approximately 15.7%, 21.3% and 26.6%, respectively. Additionally, the linear regression coefficients between S_ϕ and ϕ is −0.824, with Pearson correlation coefficient of 0.55 at a significant level ($p < 0.001$). This result suggests that the larger the aridity index basins or more arid regions, the greater sensitivity of streamflow to climate change. The one-way ANOVA and Mann-Whitney *U* test also suggest there are significant differences in sensitivity between any of the two climate regions (Table 3, $p < 0.000$). Particularly for comparing EL versus WL, the *F* and *Z* values are 54.83 and −6.20, respectively, which indicates remarkably higher sensitivity of streamflow to aridity index in the WL condition than that in EL condition.

Table 2
Statistical test for the difference of parameter *n* in three climate regions.

	One-way ANOVA test		Mann-Whitney *U* test	
	F value	*p*	*Z* value	*p*
EL vs. EQ	11.54	0.001*	3.398	0.001*
EQ vs. WL	3.344	0.070	2.878	0.004*
EL vs. WL	25.69	0.000**	4.677	0.000**

Note: EL, EQ, WL represent energy-limited, equitant and water-limited basins, respectively.
* Significant at 0.01 level.
** Significant at 0.001 level.

4.3. Relative contribution of aridity index to streamflow

Table 4 shows numbers of basin with increasing and decreasing trends for aridity index and streamflow in EL, EQ and WL regions. For the aridity index, in the EL region, there are 29 basins showing decreasing trends (nine basins significantly decreasing) and three basins increasing trends. This result indicates that the climate in most humid basins (90% humid basins) become wetter. For the EQ region, there are more basins showing decreasing trends than increasing trends.

The number of basins with decreasing trends is 36 (approximately 65% of total basins) with two basins significantly increasing; 19 basins have increasing trend with one basin significantly increasing. By contrast, in the WL region, there are more basins with increasing trend (31 basins with two significant) than the basins with decreasing trend (26 basins, approximately 45%). For the streamflow, in the EL region, there are 24 basins (75% humid basins) showing increasing trends with two basins significantly increasing, and eight basins showing decreasing trends with no significance. For the EQ condition, approximately 40% basins show increasing trends (22 basins), with nine of 33 significant basins showing decreasing trends. Particularly in the WL condition, there are 37 basins exhibiting decreasing trends (20 basins are significant), whereas only 35% basins show increasing trend. The trends of the aridity index and streamflow in the EL, EQ and WL regions consistently suggested that the wet region is getting wetter and the dry region is getting drier. In other words, the wet region has experienced decreasing aridity index but increasing streamflow and for the dry region increasing aridity index and decreasing streamflow.

To investigate responses of streamflow to aridity index in the three climate regions, Fig. 7 shows the relative contribution of aridity index to streamflow change (RC_ϕ) in these climatic regions. To clarify the indication of RC_ϕ, will give some more explanation. For example, a decrease of ϕ cause an increase of streamflow by 100 mm. Meanwhile, the other factors (such as deforestation or soil conservation measures) cause an increase of streamflow by 50 mm. Combined with the two factors, the observed streamflow will increase by 150 mm, and relative contribution of aridity index to streamflow (RC_ϕ) is approximately 66.7% (i.e., 100/150 × 100%). By contrast, if the other factors (such as

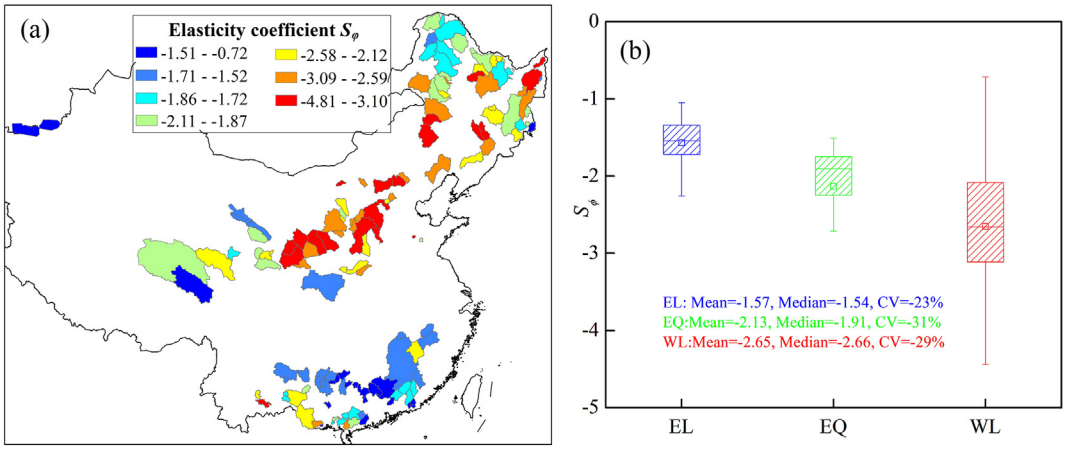

Fig. 6. (a) Spatial distribution of sensitivity coefficient in the 144 basins and (b) comparison grouped by energy-limited (EL), equitant (EQ) and water-limited (WL) regions.

drawing water from river, water transfer across river basins or vegetation consumption) cause a decrease of streamflow by -50 mm, the observed streamflow will just increase 50 mm and the *RC_ϕ* becomes 200% (i.e., 100/50* × 100%). Thus, given the other factors cause an increase (decrease) streamflow <100 mm, the *RC_ϕ* will be between larger than 50%, which demonstrate that climate change is the dominant factor to streamflow variation. However, when the other factors cause an increase (decrease) streamflow >100 mm, the *RC_ϕ* will be between negative infinity and 50%, which indicates the climate contribution to streamflow is offset by other factors and dominated by non-climatic factors.

In the EL region, the *RC_ϕ* in 75% of basins is larger than 50% (Fig. 7a), which indicates that the change of aridity index is the dominant factor to streamflow variation in most humid regions. The median value of *RC_ϕ* is approximately 79.9% (10th percentile, −50.7%; 90th percentile, 142.2%), while the other factors contribute about 20.1% to the streamflow variation. In the EQ region, there are about 55.4% of basins with *RC_ϕ* value larger than 50%, demonstrating that both of aridity change and no-climate factors exert equivalent impact on streamflow for such semi-humid or semi-arid regions. The median *RC_ϕ* value is about 55.5% (10th percentile, −42.4%; 90th percentile, 172.1%), slightly higher than other factors, while the contribution of other factors to streamflow variation also is remarkable (approximately 44.5%). By contrast, there are only 30.4% of basins with *RC_ϕ* values larger than 50% in the WL region, which indicate that just only a small proportion of basins in streamflow dominate by the aridity index, while most of basins by non-climatic factors (such as basin conditions or vegetation change). Statistics shows that the median *RC_ϕ* value is only 5.1% (10th percentile, −86.2%; 90th percentile, 147.8%), thus the contribution of non-climate factors to streamflow is approximately 94.9%. Overall, the effect of climate change on streamflow has been offset by non-climate factors. The non-climatic factors, such as human activities (Liang et al., 2015) and vegetation change (Jackson et al., 2005), dominate the variation of streamflow in the WL region.

5. Discussion

5.1. Comparison with previous work

Previous studies have reported the responses of hydrological cycle to climate change in different climatic regions (Table 5). For example, in the water-limited northwest China, Dong et al. (2014) found that the streamflow reduction caused by climate change (precipitation and *PET*) accounting for 14.3%, which suggested human activities or other factors were the major driver for streamflow variations. On the contrary, Ma et al. (2008) found that climate variability accounted for over 64% of the reduction in mean annual streamflow. Different contribution also found in the studies of Chen et al. (2013) and Tao et al. (2011). In EQ regions, Jiang et al. (2011) and Liu et al. (2012b) revealed that climate change were the main contributor to streamflow in Laohahe and Hanjiang river, while human activities dominated in Kuye and Fen river basins (Liang et al., 2013; Zhang et al., 2013). In energy-limited regions, while the Hoeya and Xinan River basins were found to be dominated by climate conditions (Xiao et al., 2018; Kim et al., 2013), the Krishna River basin was found to be dominated by human activities (Bouwer et al., 2006). As most of the previous work focus on a single river basin, there is no consensus on how climate change influence streamflow in different climate regions. For the first time, in this study, we comprehensively analyzed the contribution of climate change to streamflow based on 144 river basins covering three climate regions over China. We found that the streamflow, in WL region, was more sensitive to climate change (Fig. 6) than that in EQ or EL region, and was dominated by non-climatic factors (Fig. 7). Based on these findings, we conclude that streamflow is more sensitive to climate change in the arid regions than in the semi-arid and semi-humid or humid regions; the streamflow is dominated by non-climatic factors in arid regions and by climatic factors in humid regions.

Table 3
Statistical test to the difference of sensitivity coefficient in three climate regions.

	One-way ANOVA test		Mann-Whitney *U* test	
	F value	*p*	Z value	*p*
EL vs. EQ	19.90	0.000**	−5.32	0.000**
EQ vs. WL	14.18	0.000**	−4.35	0.000**
WL vs. EL	54.83	0.000**	−6.20	0.000**

Note: EL, EQ, WL represent energy-limited, equitant and water-limited basins, respectively.
** Significant at 0.001 level.

Table 4
Number of basins with increasing or decreasing aridity index (*ϕ*) and streamflow (*Q*) trends in three climate regions.

	ϕ			*Q*		
	Decrease	Increase	Percent decrease (%)	Decrease	Increase	Percent increase (%)
EL	29 (9)	3 (0)	90	8 (0)	24 (2)	75
EQ	36 (2)	19 (1)	65	33 (9)	22 (0)	40
WL	26 (0)	31 (2)	45	37 (20)	20 (4)	35

Notes: EL, EQ, WL represent energy-limited, equitant and water-limited regions, respectively. The number in the bracket represents the basin count at a significant level of 0.05.

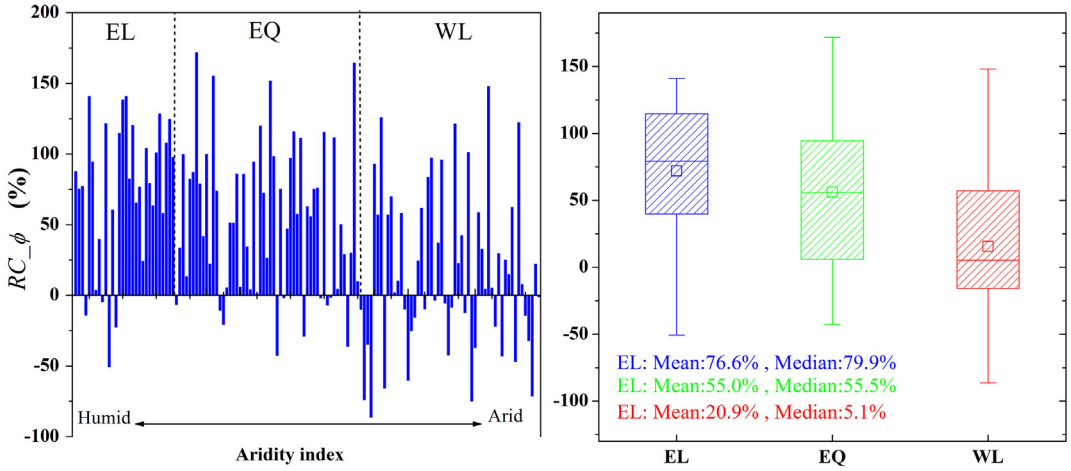

Fig. 7. Relative contribution of aridity index to streamflow (RC_ϕ) in three climate regions. EL, EQ, WL represent energy-limited, equitant and water-limited basins, respectively.

5.2. Impact of aridity index variation on water resource

The aridity index is an efficient hydro-climatic indicator (Budyko, 1974) measuring the ratio of precipitation to evapotranspiration, which indicates water availability. The deceasing trend of the aridity index was occurred in most river basins over the energy-limited region (Table 4), which would cause more precipitation into streamflow and increase the water resources in those humid basins. The increasing trends of aridity index and large sensitivity coefficient of streamflow to aridity index were identified in most river basins over the water-limited region (i.e. semi-arid and arid area). The increasing aridity index could cause more evaporation into the atmosphere, and would finally reduce the streamflow in the river and impact the water availability for livelihood and crops. Overall, the climate in EL, EQ and WL regions generally follows the pattern of "wet-get-wetter, dry-get-drier" (Greve et al., 2014), which could bring more chances for development in EL regions, while it may bring disaster to the vulnerable survival environment in the semi-arid or arid areas.

Under the changing environment, the change of aridity index could cause some new challenges to water resources in the future. Zhang et al. (2013c) documented that the potential evapotranspiration will increase by 8.67–21.27% during 2080s in three climate regions, which could increase the aridity index, decrease streamflow and aggravate water shortage, especially in the arid region. Taking the Loess Plateau (belonging to water limited region) as an example, GCMs projections show that the precipitation will decrease, in combination with an increase of potential evapotranspiration during 2011–2050 (Zhang et al., 2018c), and finally cause increase in aridity index. This suggests that the climate in the Loess Plateau will be drier in the future, and the ecological restoration project started in 1999 (Feng et al., 2016) may be challenged due to the water stresses.

5.3. Implication for water resource management in different climate regions

Water resources are rich in the south and scarce in the north of China (Table 1). The spatial heterogeneity of water resources distribution has seriously limited the economic development in north China (Liu et al., 2001). To mitigate uneven distribution of water resources between south and north China, various water resources managements were implemented, such as water diversion across river basins (Hanak et al., 2011) and reservoir constructions (Ye et al., 2003). For example, the Chinese government has implemented the South to North Water Diversion Project to transfer water from the Yangtze River (in the EL region) to Northern China (in the WL region) (Stone and Jia, 1999). Our study shows that climate change has become the dominant factor for streamflow in most humid basins (Fig. 7), thus the implementation of water diversion must be cautious when the aridity index changes in the energy limited region. Without considering the difference of hydrological response to climate change in different climate regions, the water diversion will aggravate the downstream environment problems and probably lead to an environmental disaster. The reservoir construction affects water availability. Mao et al. (2016) reported that the newly built reservoirs increased the terrestrial water storage, and reduced the observed streamflow. Constructing large reservoirs in the water-limited region may aggravate water stress in this region.

As is shown in Fig. 7, human activities have dominated the streamflow change in water-limited environments. As a result, the large-scale ecological restoration project, as one of the most important forms of human activities in the WL region, must be cautiously design with consideration of climate change (Wang et al., 2016). For example, while larger-scale afforestation in water-limited conditions will inevitably exacerbate water scarcity (Chen et al., 2015), afforestation in

Table 5
Summary of related studies about impact of climate change on streamflow. The symbol "n.g." represents to "not given".

ID	Author	River name	Climate condition	Time range	Contribution rate (%)	Dominant factor
1	Dong et al. (2014)	Jinghe River	Arid	1981–2008	14.3	Human activities
2	Ma et al. (2008)	Shiyang River	Arid	1950–2005	64	Climate change
3	Tao et al. (2011)	Tarim River	Arid	1952–2008	n.g.	Human activities since the 1970s
4	Chen et al. (2013)	Kaidu River	Arid	1960–2009	90.5	Climate change
5	Jiang et al. (2011)	Laohahe River	Semi-arid	1980–2008	89–93	Climate change
6	Liang et al. (2013)	Kuye River	Semi-arid	1960–2006	27.1–40.9	Human activities
7	Zhang et al. (2013)	Fen River	Semi-arid	1957–2010	40.7–44.6	Human activities
8	Liu et al. (2012b)	Hanjiang River	Semi-humid	1951–2006	84.1–90.1	Climate change
9	Wang et al. (2013)	Haihe River	Semi-humid	1957–2000	n.g.	Human activities:3 basins; Climate change: 1 basin
10	Bouwer et al. (2006)	Krishna River	Humid	1901–2000	6–15	Human activities
11	Du et al. (2011)	Zhengshui River	Humid	1960–2003	47	Human activities
12	Kim et al. (2013)	Hoeya Rive	Humid	2011–2100	n.g.	Climate change
13	Xiao et al. (2018)	Xinanjiang River	Humid	1955–2013	n.g.	Climate change

energy-limited conditions will be benefited by reducing flooding risk and changing the seasonal allocation of streamflow in a year (Calder, 2007). Therefore, it is important to consider the trade-off between water consumption from ecological restorations and water supply in river basins across climatic gradients.

5.4. Uncertainties

The data used in this study has undergone rigorous quality control, including correction to measurement error in the precipitation and optimized parameters a_s and b_s. However, uncertainties associated with the data may still exist. Firstly, based on the Budyko hypothesis, several equations have been derived from the Budyko's framework (Zhang et al., 2001; Yang et al., 2008; Fu, 1981; Choudhury, 1999; Roderick and Farquhar, 2011). The Chourdhury-Yang equation was the only one that was selected in this study, the equation choice may induce uncertainties in the follow-up analysis. On the other hand, several studies have documented that different equations shared the same pattern curve with no significant difference (Liu et al., 2013; Zhou et al., 2015a). The uncertainty cause by equation choice can be limited. Secondly, some basins located in the alpine region were selected (such as the headwater of Yangtze River and Tarim River in Fig. 1). The melt of snow and glacier is important hydrologic processes in these areas, and accounts for a large proportion of streamflow (Yang et al., 2015; Zhou et al., 2015b). Neglecting the meltwater from snow and glacier to the discharge can bring some limitation in the analysis. As a future work, the impact of snow and glacier change on streamflow will be studied in next work using the Gravity Recovery and Climate Experiment (GRACE) data (Liu et al., 2018). Thirdly, while Penman (1948) method is applied in this study for estimating *PET*, there are several different algorithms available (Penman, 1948; Thornthwaite, 1948; Priestley and Taylor, 1972; Monteith, 1965). The choice of *PET* estimation method may cause uncertainties in aridity index estimation. Federer et al. (1996) documented that various methods agreed well with respect to the general magnitude of the *PET* values on an annual basis over a wide range of climates.

6. Conclusions

Hydrological process and its basic components are increasingly affected by climate change and anthropogenic interference, and finally change the spatial and temporal distribution of water resources. Understanding different responses of hydrological cycle to climate change in different environmental conditions is essential for water resources management. In this paper, the response of streamflow to aridity index change were investigated in energy-limited (EL), equitant (EQ) and water-limited (WL) regions using the climate and streamflow data in 144 river basins over China. The results show that: (1) the parameter n in Choudhury-Yang's type Budyko equation exhibits significant spatial heterogeneity, with the smaller values in the EL region conditions and larger values in the WL region; (2) the mean sensitivity coefficients of streamflow to aridity index are −1.57, −2.13 and −2.65 in the EL, EQ and WL regions, respectively. This indicates that the streamflow is more sensitive to aridity index in arid river basins than that in humid river basins; (3) the median values of relative contribution rate of aridity index to streamflow is approximately 79.9%, 55.5% and 5.1% in the EL, EQ and WL regions, respectively. This suggests that climate change is the dominant factor for streamflow variation in EL and EQ, while human activities has become the major contributor to streamflow variation in the WL conditions. The implementation of water diversion and ecological restoration project should fully consider the regional difference of streamflow variation to climate change, particularly for arid and semi-arid areas with fragile ecological environments.

Acknowledgements

This study was financially supported by the National Natural Science Foundation of China (No. 41701019), the Startup Foundation for Introducing Talent of Nanjing University of Information Science & Technology (No. 2017r069), the Key Laboratory of Water Cycle and Related Land Surface Processes, Institute of Geographic Sciences and Natural Resources Research, Chinese Academy of Sciences (No. WL2017004). We also give sincerely thanks to Lifang Liu and Jiaxin Xie for providing the streamflow data. We thank the two anonymous reviewers and editors for their critical comments and constructive suggestions on the manuscript.

References

Allen, R.G., Pereira, L.S., Raes, D., Smith, M., 1998. Crop Evapotranspiration - Guidelines for Computing Crop Water Requirements - FAO Irrigation and Drainage Paper. 56. FAO.
Berghuijs, W.R., Larsen, J.R., van Emmerik, T.H.M., Woods, R.A., 2017. A global assessment of runoff sensitivity to changes in precipitation, potential evaporation, and other factors. Water Resour. Res. 53 (10), 8475–8486.
Bouwer, L., Aerts, J., Droogers, P., Dolman, A., 2006. Detecting the long-term impacts from climate variability and increasing water consumption on runoff in the Krishna river basin (India). Hydrol. Earth Syst. Sci. Discuss. 3 (4), 1249–1280.
Budyko, M.I., 1974. Climate and Life. Academic Press, New York, USA.
Calder, I.R., 2007. Forests and water—ensuring forest benefits outweigh water costs. For. Ecol. Manag. 251 (1), 110–120.
Chen, Z., Chen, Y., Li, B., 2013. Quantifying the effects of climate variability and human activities on runoff for Kaidu River Basin in arid region of northwest China. Theor. Appl. Climatol. 111 (3–4), 537–545.
Chen, Y., Wang, K., Lin, Y., Shi, W., Song, Y., He, X., 2015. Balancing green and grain trade. Nat. Geosci. 8 (10), 739–741.
Choudhury, B., 1999. Evaluation of an empirical equation for annual evaporation using field observations and results from a biophysical model. J. Hydrol. 216 (1), 99–110.
Cook, B.I., Smerdon, J.E., Seager, R., Coats, S., 2014. Global warming and 21st century drying. Clim. Dyn. 43 (9), 2607–2627.
Donat, M.G., Lowry, A.L., Alexander, L.V., O'Gorman, P.A., Maher, N., 2016. More extreme precipitation in the world's dry and wet regions. Nat. Clim. Chang. 6, 508–513.
Dong, W., Cui, B., Liu, Z., Zhang, K., 2014. Relative effects of human activities and climate change on the river runoff in an arid basin in northwest China. Hydrol. Process. 28 (18), 4854–4864.
Du, J., He, F., Zhang, Z., Shi, P., 2011. Precipitation change and human impacts on hydrologic variables in Zhengshui River Basin, China. Stoch. Env. Res. Risk A. 25 (7), 1013–1025.
Fan, H., Xu, L., Tao, H., Feng, W., Cheng, J., You, H., 2017. Accessing the difference in the climate elasticity of runoff across the Poyang Lake Basin, China. Water 9 (2), 135.
Federer, C.A., Vörösmarty, C., Fekete, B., 1996. Intercomparison of methods for calculating potential evaporation in regional and global water balance models. Water Resour. Res. 32 (7), 2315–2321.
Feng, X., Fu, B., Piao, S., Wang, S., Ciais, P., Zeng, Z., Lu, Y., Zeng, Y., Li, Y., Jiang, X., Wu, B., 2016. Revegetation in China Loess Plateau is approaching sustainable water resource limits. Nat. Clim. Chang. 6, 1019–1022.
Fu, B., 1981. On the calculation of the evaporation from land surface. Chin. J. Atmos. Sci. 5 (1), 23–31 (in Chinese).
Goodison, B., Sevruk, B., Klemm, S., 1989. WMO solid precipitation measurement intercomparison: objectives, methodology, analysis. Atmos. Depos. 179, 57–64.
Greve, P., Orlowsky, B., Mueller, B., Sheffield, J., Reichstein, M., Seneviratne, S.I., 2014. Global assessment of trends in wetting and drying over land. Nat. Geosci. 7, 716.
Guan, X., Huang, J., Guo, R., 2017. Changes in aridity in response to the global warming hiatus. J. Meteorol. Res. 31 (1), 117–125.
Hanak, E., Lund, J., Dinar, A., Gray, B., Howitt, R., Mount, J., Moyle, P., Thompson, B.B., 2011. Managing California's Water: From Conflict to Reconciliation. Public Policy Institute of California, San Francisco, Calif.
Held, I.M., Soden, B.J., 2006. Robust responses of the hydrological cycle to global warming. J. Clim. 19 (21), 5686–5699.
Hobbins, M.T., Ramírez, J.A., Brown, T.C., 2001. The complementary relationship in estimation of regional evapotranspiration: an enhanced advection-aridity model. Water Resour. Res. 37 (5), 1389–1403.
IPCC, 2013. Summary for Policymakes: The Physical Science Basis, Contribution of Working Group I to the IPCC Fifth Assessment Report Climate Change.
Jackson, R.B., Jobbágy, E.G., Roni, A., Somnath Baidya, R., Barrett, D.J., Cook, C.W., Farley, K.A., Le Maitre, D.C., Mccarl, B.A., Murray, B.C., 2005. Trading water for carbon with biological carbon sequestration. Science 310 (5756), 1944–1947.
Jaramillo, F., Destouni, G., 2015. Local flow regulation and irrigation raise global human water consumption and footprint. Science 350 (6265), 1248–1251.
Jiang, S., Ren, L., Yong, B., Singh, V.P., Yang, X., Yuan, F., 2011. Quantifying the effects of climate variability and human activities on runoff from the Laohahe basin in northern China using three different methods. Hydrol. Process. 25 (16), 2492–2505.
Kang, S., Eltahir, E.A.B., 2018. North China Plain threatened by deadly heatwaves due to climate change and irrigation. Nat. Commun. 9 (1), 2894.
Kendall, M.G., 1948. Rank Correlation Methods. Charles Griffin, London.

Kim, J., Choi, J., Choi, C., Park, S., 2013. Impacts of changes in climate and land use/land cover under IPCC RCP scenarios on streamflow in the Hoeya River Basin, Korea. Sci. Total Environ. 452-453, 181–195.
Li, Y., Liu, C., Zhang, D., Liang, K., Li, X., Dong, G., 2016. Reduced runoff due to anthropogenic intervention in the loess plateau, China. Water 8 (458), 1–16.
Li, Y., Feng, A., Liu, W., Ma, X., Dong, G., 2017. Variation of aridity index and the role of climate variables in the Southwest China. Water 9 (10), 743.
Liang, K., 2018. Comparative investigation on the decreased runoff between the water source and destination regions in the middle route of China's South-to-North Water Diversion Project. Stoch. Env. Res. Risk A. 32 (2), 369–384.
Liang, K., Liu, C., Liu, X., Song, X., 2013. Impacts of climate variability and human activity on streamflow decrease in a sediment concentrated region in the Middle Yellow River. Stoch. Env. Res. Risk A. 27 (7), 1741–1749.
Liang, W., Bai, D., Wang, F., Fu, B., Yan, J., Wang, S., Yang, Y., Long, D., Feng, M., 2015. Quantifying the impacts of climate change and ecological restoration on streamflow changes based on a Budyko hydrological model in China's Loess Plateau. Water Resour. Res. 51 (8), 6500–6519.
Liu, C., Yu, J., Eloise, K., 2001. Groundwater exploitation and its impact on the environment in the North China Plain. Water Int. 26 (2), 265–272.
Liu, X., Luo, Y., Zhang, D., Zhang, M., Liu, C., 2011. Recent changes in pan-evaporation dynamics in China. Geophys. Res. Lett. 38 (13).
Liu, C., Zhang, D., Liu, X., Zhao, C., 2012a. Spatial and temporal change in the potential evapotranspiration sensitivity to meteorological factors in China (1960–2007). J. Geogr. Sci. 22 (1), 3–14.
Liu, X., Liu, C., Luo, Y., Zhang, M., Xia, J., 2012b. Dramatic decrease in streamflow from the headwater source in the central route of China's water diversion project: climatic variation or human influence? Journal of Geophysical Research: Atmospheres 117 (D6).
Liu, X., Liu, W., Xia, J., 2013. Comparison of the streamflow sensitivity to aridity index between the Danjiangkou reservoir basin and Miyun reservoir basin, China. Theor. Appl. Climatol. 111 (3–4), 683–691.
Liu, X., Liu, C., Brutsaert, W., 2016. Regional evaporation estimates in the eastern monsoon region of China: assessment of a nonlinear formulation of the complementary principle. Water Resour. Res. 52 (12), 9511–9521.
Liu, X., Yang, T., Hsu, K., Liu, C., Sorooshian, S., 2017. Evaluating the streamflow simulation capability of PERSIANN-CDR daily rainfall products in two river basins on the Tibetan Plateau. Hydrol. Earth Syst. Sci. 21 (1), 169.
Liu, W., Sun, F., Li, Y., Zhang, G., Yan-Fang, S., Lim, W.H., Liu, J., Wang, H., Bai, P., 2018. Investigating water budget dynamics in 18 river basins across the Tibetan Plateau through multiple datasets. Hydrol. Earth Syst. Sci. 22 (1), 351.
Ma, Z., Kang, S., Zhang, L., Tong, L., Su, X., 2008. Analysis of impacts of climate variability and human activity on streamflow for a river basin in arid region of northwest China. J. Hydrol. 352 (3), 239–249.
Maliva, R.G., Missimer, T.M., 2012. Arid Lands Water Evaluation and Management. Springer Science & Business Media.
Mao, Y., Wang, K., Liu, X., Liu, C., 2016. Water storage in reservoirs built from 1997 to 2014 significantly altered the calculated evapotranspiration trends over China. J. Geophys. Res.: Atmos. 121 (17), 10,097–010,112.
McVicar, T.R., Roderick, M.L., Donohue, R.J., Van Niel, T.G., 2012. Less bluster ahead? Ecohydrological implications of global trends of terrestrial near-surface wind speeds. Ecohydrology 5 (4), 381–388.
Medhaug, I., Stolpe, M.B., Fischer, E.M., Knutti, R., 2017. Reconciling controversies about the 'global warming hiatus'. Nature 545, 41.
Monteith, J., 1965. Evaporation and Environment. p. 4.
NOAA, 2018. State of the Climate: Global Climate Report for Annual 2017. NOAA National Centers for Environmental Information, USA.
Ohmura, A., Wild, M., 2002. Is the hydrological cycle accelerating? Science 298 (5597), 1345–1346.
Penman, H.L., 1948. Natural Evaporation From Open Water, Bare Soil and Grass. The Royal Society, pp. 120–145.
Piao, S., Ciais, P., Huang, Y., Shen, Z., Peng, S., Li, J., Zhou, L., Liu, H., Ma, Y., Ding, Y., Friedlingstein, P., Liu, C., Tan, K., Yu, Y., Zhang, T., Fang, J., 2010. The impacts of climate change on water resources and agriculture in China. Nature 467 (7311), 43–51.
Priestley, C.H.B., Taylor, R.J., 1972. On the assessment of surface heat flux and evaporation using large-scale parameters. Mon. Weather Rev. 100 (2), 81–92.
Roderick, M.L., Farquhar, G.D., 2011. A simple framework for relating variations in runoff to variations in climatic conditions and catchment properties. Water Resour. Res. 47 (12).
Roderick, M.L., Greve, P., Farquhar, G.D., 2015. On the assessment of aridity with changes in atmospheric CO_2. Water Resour. Res. 51 (7), 5450–5463.
Scheff, J., Frierson, D.M., 2015. Terrestrial aridity and its response to greenhouse warming across CMIP5 climate models. J. Clim. 28 (14), 5583–5600.
Sevruk, B., Hamon, W., 1984. International comparison of national precipitation gauges with a reference pit gauge. Instruments and Observing Methods Report. 17.
Sorooshian, S., AghaKouchak, A., Arkin, P., Eylander, J., Foufoula-Georgiou, E., Harmon, R., Hendrickx, J.M.H., Imam, B., Kuligowski, R., Skahill, B., Skofronick-Jackson, G., 2011. Advancing the remote sensing of precipitation. Bull. Am. Meteorol. Soc. 92 (10), 1271–1272.
Stone, R., Jia, H., 1999. Going against the flow. Science 313 (5790), 1034–1037.
Tao, H., Gemmer, M., Bai, Y., Su, B., Mao, W., 2011. Trends of streamflow in the Tarim River Basin during the past 50 years: human impact or climate change? J. Hydrol. 400 (1), 1–9.
Thornthwaite, C.W., 1948. An approach toward a rational classification of climate. Geogr. Rev. 38 (1), 55–89.
UNESCO, 1979. Map of the World Distribution of Arid Regions: Explanatory Note. Unesco, Paris.
Wang, W., Shao, Q., Yang, T., Peng, S., Xing, W., Sun, F., Luo, Y., 2013. Quantitative assessment of the impact of climate variability and human activities on runoff changes: a case study in four catchments of the Haihe River basin, China. Hydrol. Process. 27 (8), 1158–1174.
Wang, S., Fu, B., Piao, S., Lu, Y., Ciais, P., Feng, X., Wang, Y., 2016. Reduced sediment transport in the Yellow River due to anthropogenic changes. Nat. Geosci. 9 (1), 38–41.
Wang, S., Zuo, H., Yin, Y., Hu, C., Yin, J., Ma, X., Wang, J., 2019. Interpreting rainfall anomalies using rainfall's non-negative nature. Geophys. Res. Lett. 46 (1), 426–434.
Xiao, Z., Lan, J., Li, H., Wu, Z., Luo, L., Mingyuan, C., 2018. Quantitative evaluation of contributions of climate change and underlying surface change to the runoff at the upper catchment of Xin'anjiang (Tunxi Hydrological Station). Journal of Yunnan University 40 (3), 474–482 (in Chinese).
Xing, W., Wang, W., Zou, S., Deng, C., 2018. Projection of future runoff change using climate elasticity method derived from Budyko framework in major basins across China. Glob. Planet. Chang. 162, 120–135.
Yang, H., Yang, D., 2011. Derivation of climate elasticity of runoff to assess the effects of climate change on annual runoff. Water Resour. Res. 47 (7).
Yang, D., Goodison, B., Metcalfe, J., Louie, P., Elomaa, E., Hanson, C., Golubev, V., Gunther, T., Milkovic, J., Lapin, M., 2001. Compatibility evaluation of national precipitation gage measurements. Journal of Geophysical Research: Atmospheres 106 (D2), 1481–1491.
Yang, H., Yang, D., Lei, Z., Sun, F., 2008. New analytical derivation of the mean annual water-energy balance equation. Water Resour. Res. 44 (3).
Yang, T., Wang, C., Chen, Y., Chen, X., Yu, Z., 2015. Climate change and water storage variability over an arid endorheic region. J. Hydrol. 529 (2015), 330–339.
Yang, Y., Zhang, S., McVicar, T.R., Beck, H.E., Zhang, Y., Liu, B., 2018. Disconnection between trends of atmospheric drying and continental runoff. Water Resour. Res. 54 (7), 4700–4713.
Yang, Y., Roderick, M.L., Zhang, S., McVicar, T.R., Donohue, R.J., 2019. Hydrologic implications of vegetation response to elevated CO_2 in climate projections. Nat. Clim. Chang. 9 (1), 44–48.
Ye, B., Yang, D., Kane, D.L., 2003. Changes in Lena River streamflow hydrology: human impacts versus natural variations. Water Resour. Res. 39 (7).
Ye, B., Yang, D., Ding, Y., Han, T., Koike, T., 2004. A bias-corrected precipitation climatology for China. J. Hydrometeorol. 5 (6), 1147–1160.
Ye, S., Li, H.Y., Li, S., Leung, L.R., Demissie, Y., Ran, Q., Blöschl, G., 2015. Vegetation regulation on streamflow intra-annual variability through adaption to climate variations. Geophys. Res. Lett. 42 (23), 10,307–310,315.
Zhang, L., Dawes, W., Walker, G., 2001. Response of mean annual evapotranspiration to vegetation changes at catchment scale. Water Resour. Res. 37 (3), 701–708.
Zhang, D., Liu, X., Liu, C., Bai, P., 2013. Responses of runoff to climatic variation and human activities in the Fenhe River, China. Stoch. Env. Res. Risk A. 27 (6), 1293–1301.
Zhang, D., Liu, X., Hong, H., 2013c. Assessing the effect of climate change on reference evapotranspiration in China. Stoch. Env. Res. Risk A. 27 (8), 1871–1881.
Zhang, S., Yang, H., Yang, D., Jayawardena, A., 2015. Quantifying the effect of vegetation change on the regional water balance within the Budyko Framework. Geophys. Res. Lett. 43 (3), 1140–1148.
Zhang, D., Liu, X., Zhang, Q., Liang, K., Liu, C., 2016. Investigation of factors affecting intra-annual variability of evapotranspiration and streamflow under different climate conditions. J. Hydrol. 543 (Part B), 759–769.
Zhang, D., Zhang, Q., Qiu, J., Bai, P., Liang, K., Li, X., 2018a. Intensification of hydrological drought due to human activity in the middle reaches of the Yangtze River, China. Sci. Total Environ. 637, 1432–1442.
Zhang, D., Liu, X., Bai, P., 2018b. Different influences of vegetation greening on regional water-energy balance under different climatic conditions. Forests 9 (7), 412.
Zhang, S., Yang, D., Yang, Y., Piao, S., Yang, H., Lei, H., Fu, B., 2018c. Excessive afforestation and soil drying on China's Loess Plateau. J. Geophys. Res. Biogeosci. 123 (3), 923–935.
Zheng, H., Zhang, L., Zhu, R., Liu, C., Sato, Y., Fukushima, Y., 2009. Responses of streamflow to climate and land surface change in the headwaters of the Yellow River Basin. Water Resour. Res. 45 (7), 641–648.
Zhou, S., Yu, B., Huang, Y., Wang, G., 2015a. The complementary relationship and generation of the Budyko functions. Geophys. Res. Lett. 42 (6), 1781–1790.
Zhou, J., Wang, L., Zhang, Y., Guo, Y., Li, X., Liu, W., 2015b. Exploring the water storage changes in the largest lake (Selin Co) over the Tibetan Plateau during 2003–2012 from a basin-wide hydrological modeling. Water Resour. Res. 51 (10), 8060–8086.